sustainability

Article

Assessment of Land Cover Changes and Climate Variability Effects on Catchment Hydrology Using a Physically Distributed Model

Sanjeet Kumar [1,*], Ashok Mishra [2] and Umesh Kumar Singh [1]

[1] Department of Civil Engineering, Koneru Lakshmaiah Education Foundation Deemed to be University, Guntur 522502, India; umesh.ais@gmail.com
[2] Department of Agricultural and Food Engineering, Indian Institute of Technology, Kharagpur 721302, India; amishra@agfe.iitkgp.ernet.in
* Correspondence: sanjeetiitkgp@gmail.com

Abstract: Land use/land cover, along with climate variability, play vital roles in hydrological functionality of catchments and are leading threats to inter-related hydrological processes. In the current study, a physically distributed Soil and Water Assessment Tool model is used to investigate the impact of historical changes on the hydrologic response of the Damodar catchment (Jharkhand, India) in terms of inflow to the Panchet reservoir. The model was validated for the monthly runoff and inflow at the outlets of four watersheds and three reservoirs in the Damodar catchment before the assessment of changes in inflow at the Panchet reservoir was performed. The analysis of land cover thematic maps prepared using satellite images of Landsat 4, 5 and 7 showed that from 1972 to 2001, the land cover in the Damodar catchment changed considerably. The interpretation of land cover results indicates that significant increases in settlements (140%), waterbodies (98.42%) and agricultural land (26.71%), along with decreases in wasteland (32.63%) and forest (15.28%), occurred due to development. The Mann–Kendall test was used for measuring the rainfall and temperature for the Damodar catchment, which showed that this region became drier during 1970–2005, with decreases in the annual rainfall and increases in the mean temperature. A simulated hydrological impact under land cover dynamics and climate variability in the historical time frame of 1970–2000 using the model revealed a gradual increase of 26.16% in the Panchet reservoir inflow. The study revealed that the increased inflow is relatively greater under the influence of climate variability due to changes in rainfall and temperature, rather than land cover, that were observed over the region.

Keywords: hydrological; SWAT; runoff; inflow; climate; reservoir

check for updates

Citation: Kumar, S.; Mishra, A.; Singh, U.K. Assessment of Land Cover Changes and Climate Variability Effects on Catchment Hydrology Using a Physically Distributed Model. *Sustainability* **2023**, *15*, 10304. https://doi.org/10.3390/su151310304

Academic Editors: Mukesh K. Tiwari, Deepesh Machiwal and Adlul Islam

Received: 14 December 2022
Revised: 13 April 2023
Accepted: 26 April 2023
Published: 29 June 2023

1. Introduction

Land use/land cover (LULC) and climate variability affect the hydrological response and functionality of any region by causing fluctuations in many inter-related processes, leading to clear hydrology implications for stream flow, soil erosion, sedimentation and nutrient loadings, etc., at temporal and spatial scales [1–4]. Thus, reliable evidence on the spatial and temporal distribution of LULC is needed to simulate its effect on the hydrological response. LULC changes occur for a variety of reasons [5,6] and have been studied by applying different methods, such as obtaining information from historical records, field studies and satellite imagery [7,8]. Predictions of future land cover scenarios based on initial land cover, probabilities of the possible occurrence of a given land cover change, the spatial patterns of change [9,10] and the modelling of extreme scenarios [11] have been used for the impact assessment of LULC changes on catchment hydrology.

In recent years, paired watershed designs have served as a reference for many studies [12,13], and such studies can provide direct evidence of the impacts of land use change on runoff, soil erosion, etc.; however, they generally require long time steps and cover small areas, and thus, cannot be easily applied to large catchments due to heterogeneity [14,15]. For these reasons, physically based distributed hydrological models are becoming popular and are increasingly being used to investigate the hydrological impacts of LULC changes [16–19], in which LULC properties are characterized by parameters [20]. Other approaches such as quantifying the historical–fractional changes in the land cover extent through remote sensing [6] and scenario generation using probabilistic models have been used to study the impacts of LULC change on watersheds, which serve as basic data for hydrological modeling. Particularly in regions with a high temporal variability in temperature or rainfall, the date of the satellite imagery has a pronounced impact on the identifiable and distinguishable land use classes. To derive a classification that is representative of the whole year, several land use classifications from different times in the year can be combined to produce one multitemporal land use classification [21]. By this means, the intra-annual differences are minimized and a series of such multitemporal land use classifications can be analyzed to identify the inter-annual or inter-decadal changes over a past period.

Hydrological models of different complexity are available and were established as powerful tools to quantify the hydrological responses to LULC and climate together [2,22]. The SWAT model is one such model that is extensively cited in the literature and has been adapted by many researchers to study the impacts of LULC changes and climate variability on large and small watersheds around the world [23,24]. In recent studies, the SWAT model was employed to assess the effects of LULC on hydrology [7,22,25,26]. It was applied to the Zanjanrood basin in Iran [13], the Upper Shire River basin in Malawi [27], the San Pedro watershed in Mexico [28], the Upper Du watershed in China [29] and the Hiranyakeshi watershed [19]. The above research shows satisfactory applications of the SWAT model and broadly concludes that modeling could be a useful technique for identifying sensitive areas within a river basin/watershed and for linking land cover and hydrology; it could, therefore, serve as a platform for scenario building for the management of resources in the future [30,31]. The Damodar catchment is an important area for natural resources such as forests, agricultural land and minerals; at the same time, a number of various industries, i.e., coal washeries, steelworks and thermal power plants, are located in the catchment. Moreover, the larger mining activities increased during the past few decades and have seriously affected the catchment in terms of LULC change, sedimentation, soil erosion, etc. Considering these facts and the research needed, the present study was undertaken to assess the impact of LULC and climate variability on reservoir inflow, with objectives to calibrate and validate the SWAT hydrological model for the Damodar catchment and to assess the historical changes in water availability in terms of the reservoir inflow.

2. Materials and Methods

2.1. Study Area: Damodar Catchment

The Damodar catchment is a part of the Damodar River in the Jharkhand state of India (Figure 1) in the eastern part of the country. The catchment lies between the latitudes of 23°34′0′′ and 24°91′0′′ north and longitudes of 84°42′0′′ and 86°46′0′′ east. The catchment covers an area of 10,878 km^2 with an elevation variation between 122 and 1340 m above mean sea level. Daily temperatures vary between a minimum of 3 °C and a maximum of 44 °C, with an average annual rainfall of 1250 mm over the area. Most of the rainfall occurs during the monsoon season (July to September), which accounts for more than 80% of the annual rainfall. The vegetation of the study area comprises mixed forest, mainly deciduous and tropical moist forest. There are rainfed agricultural activities, along with irrigated areas, which are supplied by multipurpose reservoirs in the catchment, including the Konar, Tenughat and Panchet reservoirs.

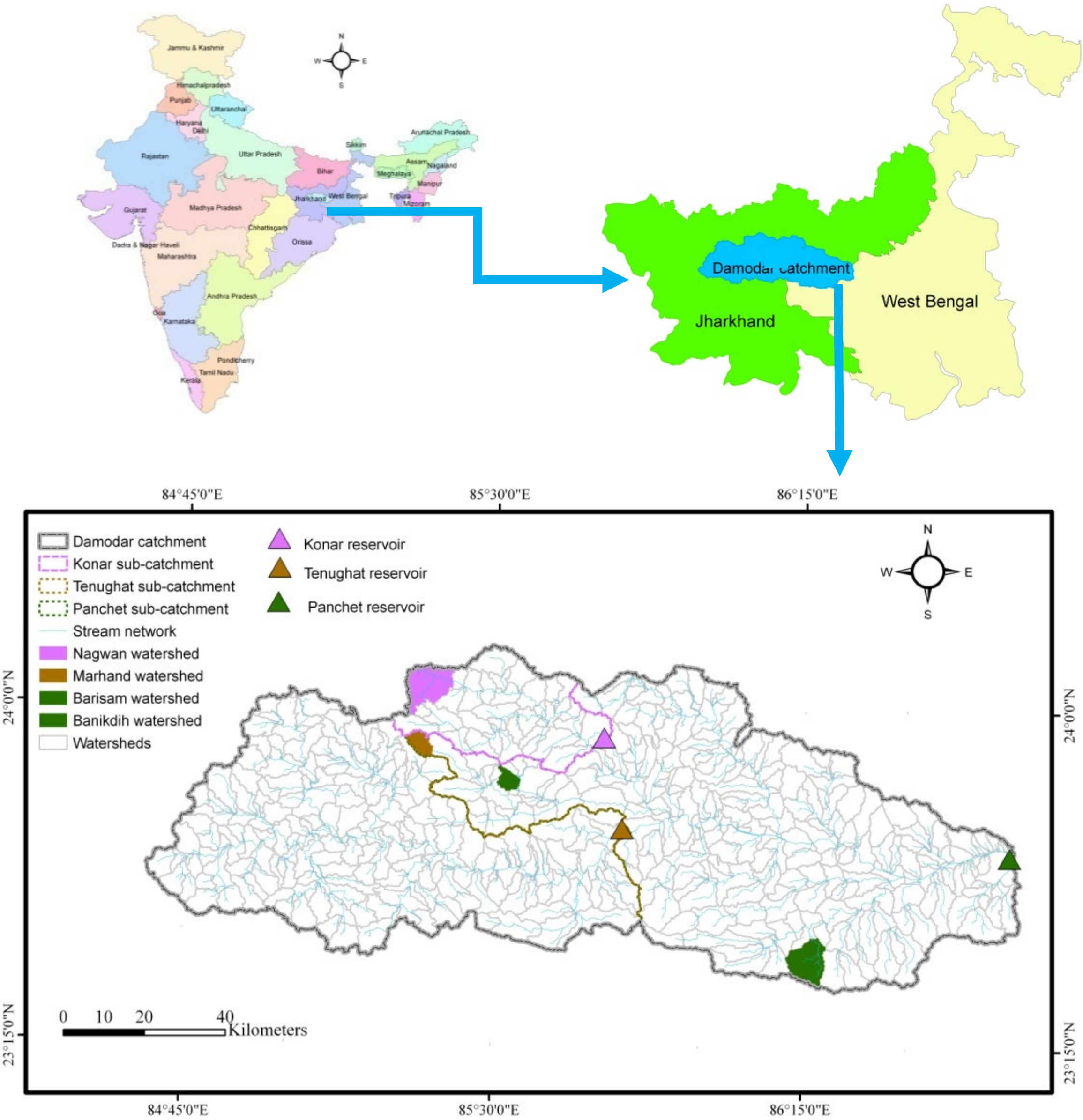

Figure 1. Location map of the study area—Damodar catchment.

2.2. Data Sets and Sources

The topography of the Damodar catchment was characterized by using digital elevation model (DEM) of 30 m resolution, prepared from the Advanced Spaceborne Thermal Emission and Reflection Radiometer Global Digital Elevation Model, available at NASA's Land Processes Distributed Archive Center (LP DAAC). The information pertaining to soils of the study area and their properties (organic matter content, bulk density, hydraulic conductivity, drainage pattern and soil hydrologic group) were collected from Damodar Valley Corporation (DVC), Hazaribagh, India. The soil coverage was classified into three texture groups—sandy loam (80.17% area), loamy sand (10.3% area) and sandy clay loam (9.53% area).

The spatial distribution of land use and land cover classes, their dynamics and temporal conversion from one to the other were studied using remote sensing images of Landsat satellite 4, 5 and 7 downloaded from Global Land Cover Facility (GLCF) for the years 1972 (Landsat 4), 1989 (Landsat 5) and 2000 (Landsat 7) using different dates.

Due to the large geographical extent and topographical variation, the area witnesses a spatial and temporal variation in the climatic and hydrological data. Although the catchment is the most extensively gauged catchment in the country, availability of various climatic and hydrological data is still scarce for many watersheds in the catchment. Girded ($1^\circ \times 1^\circ$) daily rainfall (from 1970 to 2007) and minimum/maximum temperature (from 1970 to 2005) data were collected from the India Meteorological Department (IMD) in Pune, India. Daily humidity, wind speed, solar radiation and monthly runoff for the monsoon months (from June to September) for five years (1997–2001) for four watersheds (Barisam, Banikdih, Mahrand and Nagwan) were collected from Soil Conservation Department (SCD), DVC, Hazaribagh, India. Reservoir inflow and outflow for Konar and Panchet reservoirs for the period from 1960 to 2012 were obtained from the Reservoir Operation Department, DVC, Maithon, Jharkhand, India, whereas the daily inflow and outflow of Tenughat reservoir, from 1972 to 2012, were collected from the Central Water Commission, Asansol, West Bengal, India. The Konar River joins the Damodar River near Bokaro city and finally drains into the Panchet reservoir.

2.3. Distributed Hydrologic Modeling: SWAT Model

The Soil and Water Assessment Tool (SWAT) is a semi-distributed process-based hydrological model developed by the United States Department of Agriculture-Agricultural Research Service (USDA-ARS). The model operates on a daily time step to simulate different hydrological processes at the basin/watershed level [32] to simulate quality and quantity of surface and ground water resources. The model is capable of evaluating the impact of heterogeneous soil, land cover changes, sedimentation and agricultural chemical yields on water quality and quantity. The model is well defined to route water and sediment from distinct watersheds through the river network, and has the ability to integrate water bodies, such as ponds and reservoirs, using identical methods of process modeling. For details about the model, one may refer to the SWAT user manual [33].

2.4. Model Calibration, Up-Scaling of Calibrated Parameter and Validation

The SWAT model was first calibrated by using observed monthly runoff measured at the outlets of Barisam, Banikdih, Mahrand and Nagwan watersheds during monsoon months (from June to September), for the period from 1997 to 1999. After calibration of the model, calibrated parameters were up-scaled to other ungauged watersheds of the Damodar catchment for the calibration of inflow to the Konar, Tenughat and Panchet reservoirs. The up-scaling of calibrated parameters was performed for other un-gauged watersheds of respective sub-catchments (calibrated parameters of Barisam and Banikdih were up-scaled for Panchet sub-catchment, Nagwan was up-scaled for Konar sub-catchment and Mahrand was up-scaled for Tenughat sub-catchment for the calibration of reservoir inflow). Calibration of Tenughat and Konar reservoir was performed first, and then calibration of Panchet reservoir was performed, as the outflow of Tenughat and Konar are the inflow of the Panchet reservoir. After calibration for runoff at the outlet of four watersheds and reservoir inflow, the calibrated parameters were kept constant for model validation to simulate runoff and reservoir inflows for the period from 2000 to 2001. During the calibration and validation period, an initial warm-up period of two years was taken to ensure normalized initial process in model simulation. The model performances during the calibration and validation processes were evaluated by analyzing the statistical parameters—Nash–Sutcliffe efficiency (NSE), coefficient of determination (R^2), root mean square error (RMSE) and percent bias (PBIAS)—as goodness of fit criteria, recommended by the American Society of Civil Engineers (ASCE) 1993 [34].

2.5. Trend Analysis of Historical Meteorology Data

The spatial and temporal trend analysis of the annual and monthly rainfall and temperature information, collected from IMD as grid data over Damodar catchment for the period 1970–2005, was performed using Mann–Kendall (MK) test [35]. The test was applied to quantify the significance and magnitude of monotonic trends in hydro-meteorological time series. The Damodar catchment is covered by five grids of IMD data—DVC1 (latitude

23.5 north—longitude 84.5 east), DVC2 (latitude 23.5 north—longitude 85.5 east), DVC3 (latitude 23.5 north—longitude 86.5 east), DVC4 (latitude 24.5 north—longitude 85.5 east), DVC5 (latitude 24.5 north—longitude 86.5 east)—that were used for the analysis.

2.6. Impact of LULC Change and Climate Variability on Damodar Catchment

To evaluate the impact of historical LULC change and climate variability on the Damodar catchment hydrology, the approach of one factor at a time was used (i.e., changing one factor at a time while holding other factors constant). Meteorological data of the three decadal climate information, i.e., time slices of 1971–1980, 1981–1990 and 1991–2000, were selected, and each time slice included one LULC map. The LULC maps of 1972, 1990 and 2000 were used to represent the LULC patterns of 1970s (1971–1980), 1990s (1981–1990) and 2000s (1991–2000), respectively. The calibrated and validated SWAT model was run for each of the nine combinations of three LULC and three time slices, forming a total of nine scenarios. The influences of the LULC change and climate variability were quantified by comparing the SWAT outputs of the nine combination scenarios for the Panchet reservoir in terms of reservoir inflow as follows: T1—1972 LULC map and 1971–1980 climate; T2—1990 LULC map and 1971–1980 climate; T3—2001 LULC map and 1971–1980 climate; T4—1972 LULC map and 1981–1990 climate; T5—1990 LULC map and 1981–1990 climate; T6—2001 LULC map and 1981–1990 climate; T7—1972 LULC map and 1991–2000 climate; T8—1990 LULC map and 1991–2000 climate; T9—2001 LULC map and 1991–2000 climate.

3. Results and Discussion

3.1. Land Use/Land Cover Classification

The historical LULC dynamics of the Damodar catchment were prepared from the satellite images of Landsat 4 (1972), 5 (1990) and 7 (2001) and separated into the following five major classes: settlement, forest, water bodies, agricultural land and wasteland. The accuracy assessment of the classified image was performed only for Landsat 7 and subsequently used for the classification of the Landsat 4 and Landsat 5 images. The overall classification accuracy (84.50%) and Kappa statistics (0.81) of Landsat 7 indicate that the accuracy is reasonably good and may be used for further study. The LULC change from 1972 to 2001 was studied, and the area under different land cover classes during this period is shown in Figure 2. The figure reveals that agriculture (39.38%) and forest (27.11%) land were dominant in the study area during the year 2001. The analysis shows a good percent increase in settlement (140%), water bodies (98.42%) and agricultural land (26.71%) that took place in the catchment from 1972 to 2001. On the other hand, the forest and wasteland decreased, respectively, by 15.28% and 32.63% during the same period. The increase in the water bodies' area may be because of the construction of water storage structures like ponds, check dams and the increase in the water storage level of reservoirs in the catchment. The increase in the settlement area is due to the increase in mining activities, which consequently increased the population in the catchment, particularly in the Tenughat and Panchet sub-catchment.

3.2. Calibration and Validation of SWAT Model

The SWAT model was calibrated (1997–1999) and validated (2000–2001) at the outlets of four watersheds (Nagwan, Mahrand, Barisam and Banikdih) using the observed monthly runoff during the monsoon period and the observed reservoir inflow at three reservoirs (Konar, Tenughat and Panchet) during both the monsoon and non-monsoon periods. The calibrated parameters, based on the sensitivity analysis for the four watersheds, are shown in Table 1. The results of the model calibration and validation for runoff and reservoir inflows are presented below.

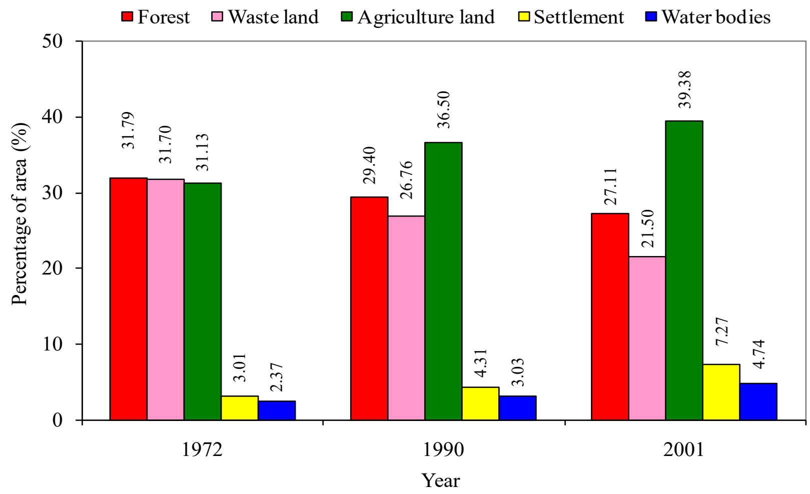

Figure 2. Percentage of total land cover under different LULC classes in the Damodar catchment during 1972, 1990 and 2001.

Table 1. Calibrated parameter values for the Barisam, Banikdih, Mahrand and Nagwan watersheds.

Model Parameter	**Prescribed Range**		**Barisam**	**Banikdih**	**Mahrand**	**Nagwan**
	Minimum	**Maximum**				
OV_N	0.01	30	0.15	0.07	0.20	0.10
CH_N1	0.01	30	0.15	0.21	0.18	0.09
CH_K1	0	300	2.15	6.70	2.50	2.00
CH_N2	0.01	0.3	0.15	0.19	0.01	0.04
CH_K2	0	300	1.00	1.00	1.00	3.00
SURLAG	0	10	1.00	1.00	1.00	1.00
CN2	35	98	49–79	73–81	48–67	49–67
ALPHA_BF	0	1	0.5	0.5	0.5	0.5
CH_EROD	0	1	0.5	0.5	0.5	0.5
CH_COV	0	1	0.5	0.5	0.5	0.5
SPCON	0	0.01	0.009	0.009	0.009	0.009
SPEXP	1	2	1.13	1.13	1.13	1.13
USLE_P	0	1	0.8	0.6	0.8	0.6
ALPHA_GW	0	1	0.3	0.3	0.3	0.3
EPCO	0	1	0.6	0.6	0.6	0.6
ESCO	0	1	0.5	0.5	0.5	0.5

3.3. Runoff: Calibration and Validation

The graphical comparisons of the monthly measured and simulated runoff from the four watersheds (Barisam, Banikdih, Mahrand and Nagwan) are presented in Figure 3 for monsoon season during the calibration and validation periods. The figure shows that the magnitude and temporal variation of the simulated monthly runoff follow the pattern of measured runoff from the four watersheds during monsoon season. The results also show that during high rainfall in some months, the runoff is over- as well as slightly underestimated by the model for all four watersheds. This may be due to the low initial soil moisture and higher storage loss condition. However, the overall graphical comparison of the model's performance is satisfactory, as indicated by the close agreement between the measured and simulated runoff from the four watersheds. In order to compare the model simulation with the measured counterpart, statistical analyses were performed during the calibration and validation periods.

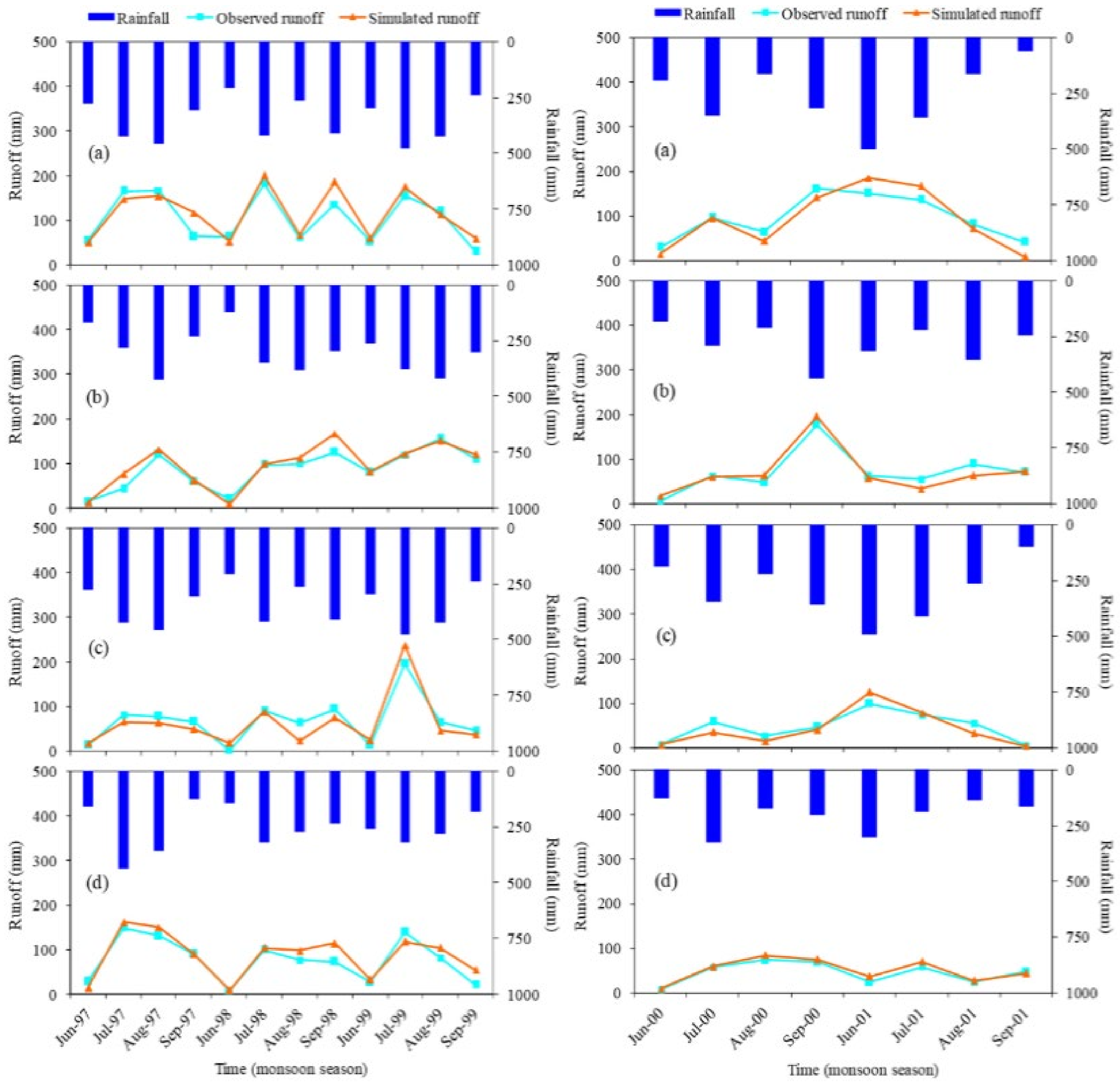

Figure 3. Comparison between measured and simulated monthly runoff during calibration and validation periods at the outlets of (**a**) Barisam, (**b**) Banikdih, (**c**) Mahrand and (**d**) Nagwan watersheds.

Statistical tests were performed to compare the simulated monthly runoff and reservoir inflows with their measured counterpart, and the results are presented in Table 2. The statistical test results show a close linear relationship between the measured and simulated runoff during the calibration period with R^2 values of 0.83, 0.91, 0.89 and 0.87 for the Barisam, Banikdih, Mahrand and Nagwan watersheds, respectively. The NSE values of 0.77, 0.84, 0.82 and 0.80 for the Barisam, Banikdih, Mahrand, and Nagwan watersheds, respectively, also show a better agreement between the peaks of the measured and simulated runoff. On the other hand, low RMSE values varying between 16.83 and 25.30 mm and low PBIAS values from −7.64% to 13.65 for the four watersheds reflect a close agreement between the measured and simulated runoff. The low value of the PBIAS indicates that the model predicts monthly runoff, from the four watersheds, within the acceptable limit of accuracy during the calibration period, as suggested by Moriasi et al. (2007) [36].

Table 2. Statistical analysis between measured and simulated monthly runoff for watersheds and reservoir inflow during calibration and validation periods.

Statistical Parameters	Barisam		Banikdih		Mahrand		Nagwan		Konar		Tenughat		Panchet	
	Cali.	**Vali.**	**Cali.**	**Vali.**	**Cali.**	**Vali.**	**Cali.**	**Vali.**	**Cali.**	**Vali.**	**Cali.**	**Vali.**	**Cali.**	**Vali.**
R^2	0.83	0.93	0.91	0.91	0.89	0.87	0.87	0.95	0.82	0.81	0.85	0.89	0.86	0.96
NSE	0.77	0.76	0.84	0.88	0.82	0.74	0.80	0.87	0.80	0.76	0.84	0.87	0.86	0.93
RMSE (mm)	25.30	23.06	16.83	15.50	20.76	15.52	20.36	7.60	9.73	7.84	54.09	43.16	93.90	50.95
PBIAS (%)	10.87	−4.21	9.63	−1.01	−7.64	−9.76	13.65	12.33	9.42	−8.21	4.03	5.74	−1.79	16.77

It is observed from Table 2 that the R^2 values vary between 0.87 and 0.95 and the NSE values vary between 0.74 and 0.88, indicating a close linear relationship between the observed and simulated monthly runoff. The closer values of R^2 and NSE indicate that the model simulated the runoff pattern and magnitude quite accurately during the validation period. The RMSE values between 7.60 and 23.06 mm and PBIAS values of −9.76% to 12.33%, respectively, for the watersheds indicate a close agreement between the measured and simulated monthly runoff. The value of PBIAS indicates that the model is under predicting the runoff for Barisam, Banikdih and Mahrand and over predicting the runoff for Nagwan. However, the under and over prediction of runoff from the watersheds are within the acceptable limit of accuracy during the validation period, as suggested by Moriasi et al. (2007) [36].

3.4. Reservoir Inflow: Calibration and Validation

The graphical comparison between the measured and simulated inflow to the Konar, Tenughat and Panchet reservoirs for the calibration and validation periods are shown in Figure 4. The calibration and validation of the reservoirs' inflow were performed for both monsoon and non-monsoon season. From the graphical comparison, it is observed that the simulated monthly inflows matched well with their measured counterparts of the three reservoirs. However, the model under and over predicted the inflow in all three reservoirs during the start of the calibration and validation periods; this may be due to the reservoirs' initial and temporal storage and soil moisture conditions in the reservoir catchments. The variation may also be attributed to the use of five rainfall grids of IMD data for simulating the hydrological processes in the large catchment area (10,878 km^2), divided into 411 watersheds, which may have not captured the spatial and temporal variability of rainfall over the area well. Overall, the simulated inflow to the Konar, Tenughat and Panchet reservoirs are well simulated by the model during the calibration and validation periods.

Table 2 presents the statistical comparison between the measured and simulated inflow during the calibration and validation periods for the three reservoirs. The statistics indicate a close agreement between the measured and simulated inflow to the three reservoirs with quite high values of R^2 (0.82 to 0.86) and NSE (0.80 to 0.86) for the calibration period. During calibration, the total inflow to the Konar and Tenughat reservoirs is over predicted and is slightly under predicted in the case of the Panchet reservoir. The under prediction of inflow into the Panchet reservoir may be due to the presence of the Konar and Tenughat reservoirs and other water harvesting structures like check dams, farm ponds, etc., in the upstream area. Although the outflow from the Konar and Tenughat reservoirs are considered in this study, the unavailability of data pertaining to other water harvesting structures may be the one reason for the under and over prediction in the total inflow into the three reservoirs. The low RMSE values (from 9.73 m^3/s to 93.90 m^3/s) and low PBIAS (from −1.79% to 9.42%) for the Konar, Tenughat and Panchet reservoirs reflect a close agreement between the observed and model-simulated inflows. At the same time, the results of the statistical tests performed for the validation periods (Table 2) also indicate an appropriate simulation of pattern and magnitude of inflow into the three reservoirs, with quite high values of R^2 (0.81 to 0.96) and NSE (0.76 to 0.93). The model under predicted the total inflow (8.21%) to the Konar reservoir and over predicted the total inflow for the Tenughat (5.74%) and Panchet (16.77%) reservoirs, but overall, the PBAIS are within reasonable limits, as described by Moriasi et al. (2007) [36]. The low value of RMSE also indicates a good agreement between the measured and simulated inflow. Based on the above results, it can be said that the SWAT model well simulates the hydrological processes of the four watersheds and three reservoirs in the Damodar catchment and can be used for further study.

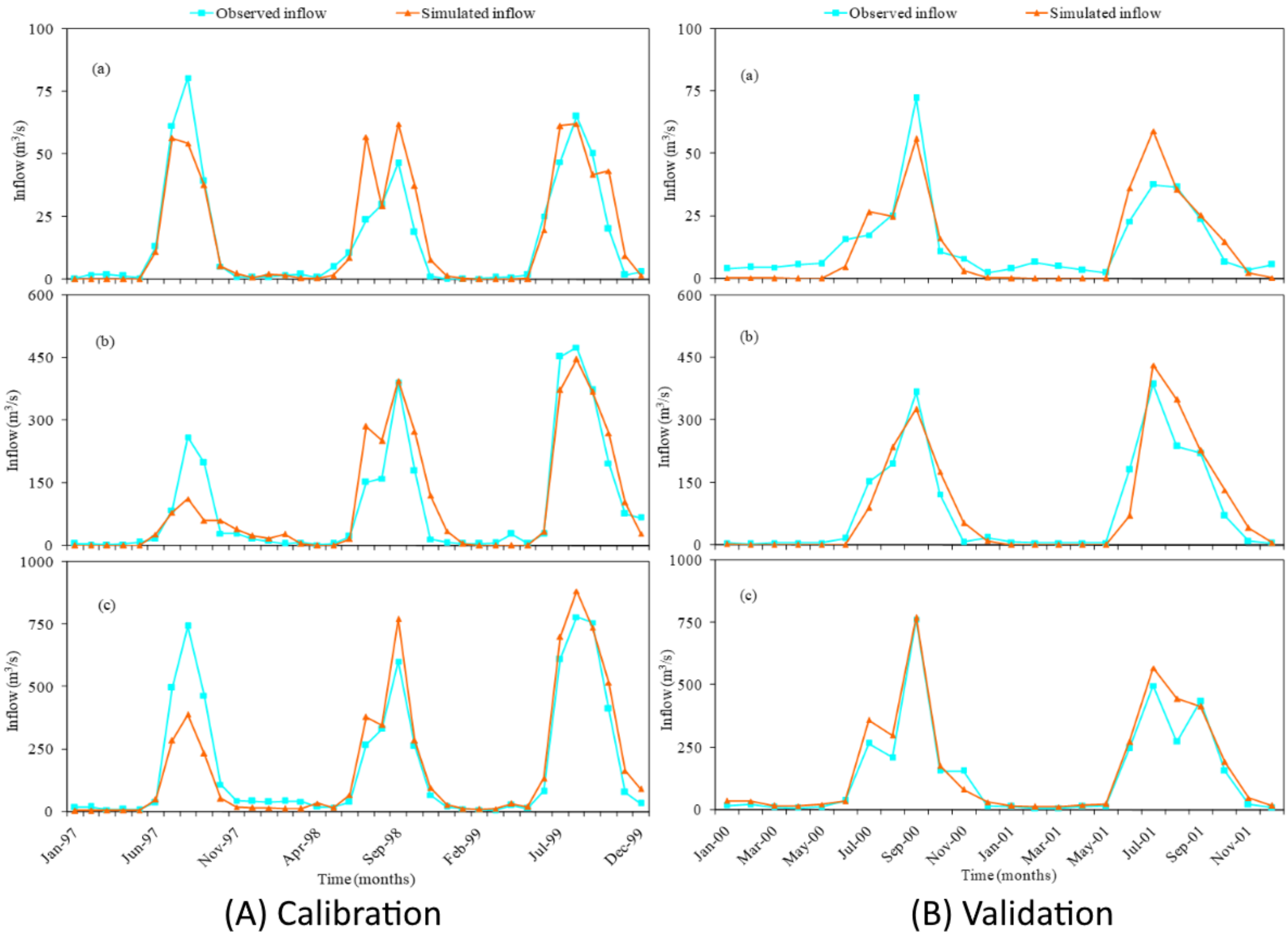

Figure 4. Measured and simulated monthly inflow during calibration and validation periods for (**a**) Konar, (**b**) Tenughat and (**c**) Panchet reservoirs.

3.5. Climate Variability: Trend Analysis of Temporal Variability

The trend analysis was performed using the Mann–Kendall non-parametric test to discover the existence of a trend in the data series (rainfall and temperature during 1970–2005) of five IMD grids (DVC1, DVC2, DVC3, DVC4 and DVC5) covering the Damodar catchment. The results for the annual trend of the rainfall and the minimum and maximum temperatures are given in Table 3. The results of the Mann–Kendall test for the annual rainfall for grids DVC1, DVC2 and DVC4 show a decreasing trend, while the results for the DVC3 and DVC5 grids show an increasing trend; however, these trends are not statistically significant at a 10% level of confidence ($p < 0.1$). On the other hand, the mean annual maximum temperatures for grids DVC1, DVC2 and DVC4 show an increasing trend, while the DVC3 and DVC5 grids show a decreasing trend over the Damodar catchment. The mean maximum temperature follows the opposite trend as that of the rainfall over the Damodar catchment, but this trend is not statistically significant ($p < 0.1$). The decreasing trend in the maximum temperatures (DVC3 and DVC5) was found because of the increasing trend in the rainfall over the catchment (DVC3 and DVC5) and vice versa for grids DVC1, DVC2 and DVC4. The analysis of the mean annual minimum temperature over the region shows that the minimum temperature increased during 1970–2005. The mean annual minimum temperatures for grids DVC2, DVC3 and DVC5 show an increasing trend, but are only statistically significant ($p < 0.05$) for grids DVC3 and DVC5, while grids DVC1 and DVC4 show a decreasing insignificant ($p < 0.1$) trend. Overall, from the annual trend analysis, it was found that the Damodar region became dryer during 1970–2005 because of the decreased annual rainfall and the increased mean annual maximum and minimum temperatures.

Table 3. Results of trend analysis for annual rainfall, mean annual maximum and minimum temperatures using Mann–Kendall nonparametric test.

Grid	Annual Rainfall			Mean Annual Maximum Temperature			Mean Annual Minimum Temperature		
	B	Z	*p*	β	Z	*p*	B	Z	*p*
DVC1	−0.666	−0.095		0.009	1.008		−0.011	−1.635	
DVC2	−2.140	−0.422		0.002	0.300		0.000	0.027	
DVC3	3.184	0.640		−0.009	−0.953		0.015	2.724	**
DVC4	−5.866	−1.430		0.000	0.014		−0.010	−1.376	
DVC5	12.298	1.321		−0.007	−0.477		0.016	3.337	**

Note: ** indicates mean significance levels at $p < 0.05$; Z is statistics of Mann–Kendall test; β is the slope estimator.

The trend analysis for the mean monthly rainfall was also performed, and the results are presented in Table 4. The mean monthly rainfall analyses for most of the months for grids DVC1, DVC2 and DVC4 show a decreasing trend, and for grids DVC3 and DVC5, they show an increasing trend over the region but are not statistically significant, except for January and June for grid DVC5 ($p < 0.05$). During the winter season (December, January, February and March), the mean monthly rainfall for January and February show a decreasing but statistically insignificant trend for all grids except for grid DVC5 in the month of January, which is significant ($p < 0.05$). The rainfall during December shows an increasing trend for grids DVC1, DVC2 and DVC3 and a decreasing trend for grids DV4 and DVC5. A decreasing trend, though statistically insignificant, in the mean monthly rainfall for March was observed over the region.

Table 4. Results of trend analysis for mean monthly rainfall using Mann–Kendall nonparametric test.

Month	DVC1			DVC2			DVC3			DVC4			DVC5		
	β	Z	*p*	B	Z	*p*	β	Z	*p*	β	Z	*p*	β	Z	*p*
Jan	−0.190	−0.913		−0.108	−0.599		−0.094	−0.627		−0.056	−0.899		−0.214	−2.384	**
Feb	−0.375	−1.403		−0.122	−0.504		−0.133	−0.395		−0.010	−0.286		−0.058	−1.389	
Mar	0.024	0.313		−0.048	−0.232		0.000	−0.054		0.000	−0.354		0.000	−0.272	
Apr	−0.265	−1.131		−0.217	−0.804		−0.002	−0.014		−0.035	−0.490		−0.035	−0.899	
May	0.033	0.068		−0.271	−0.449		0.274	0.313		−0.185	−0.504		0.395	0.586	
Jun	1.750	1.240		2.976	1.566		2.205	1.267		−0.295	−0.150		4.488	2.193	**
Jul	−0.303	−0.204		−1.925	−1.212		0.666	0.395		−2.190	−0.940		1.906	0.804	
Aug	0.034	0.027		−1.613	−0.776		0.432	0.327		−1.779	−0.885		3.406	1.321	
Sep	−0.400	−0.286		−2.013	−0.994		−0.058	−0.068		−0.993	−0.667		1.252	0.313	
Oct	0.710	0.722		0.215	0.232		0.917	0.804		−1.343	−1.471		1.098	0.558	
Nov	0.000	−0.504		0.000	0.204		0.000	−0.817		0.000	0.000		0.000	−1.240	
Dec	0.000	0.368		0.000	0.463		0.000	0.640		0.000	−0.368		0.000	−0.708	

Note: ** indicates mean significance levels at $p < 0.05$; Z is statistics of Mann–Kendall test; β is the slope estimator.

During monsoon season (from June to September), grids DVC2 and DVC4 show a decreasing trend, and grids DVC1, DVC3 and DVC5 show an increasing trend in the mean monthly rainfall. But the trend is not statistically significant ($p < 0.05$) for any month except for June for grid DVC5. It is observed from the monthly analysis that there is a statistically insignificant decrease in the rainfall in the month of September over the region. During the post-monsoon months (ON), an increase in the mean monthly rainfall is observed in the month of October for grids DVC1, DVC2, DVC3 and DVC5, and a decreasing trend is observed for grid DVC4. In the month of November, an increase in rainfall is observed for grid DVC2, and a decrease is observed for grids DVC1, DVC3 and DVC5, but is not found to be statistically significant either in November or December. During the summer season (April and May), an insignificant decrease in the rainfall is analyzed for the month of April for all the grids, whereas the May rainfall shows an insignificant increase in grids DVC1, DVC3 and DVC5, and an insignificant decrease in grids DVC2 and DVC4. Overall, from the all-month analyses, it was found that there was a decrease in the rainfall during the winter and summer seasons over the region during 1970–2005, with a slight variation during the monsoon and post-monsoon seasons.

The results of the Mann–Kendall test for the mean monthly maximum temperature are presented in Table 5. During monsoon season (June, July, August and September), all the grids show an increase in the mean monthly maximum temperature, except for the months of June (DVC1, DVC2 and DVC4) and July (DVC1, DVC4 and DVC5). This may be due to the decrease in rainfall during monsoon season. During the post-monsoon months (October and November), a decrease in the temperature was found in the month of October for all the grids, which was significant only for grid DVC3. On the other hand, November shows an increasing (statically significant at grid DVC1) trend for all the grids except in the case of grid DVC3. During the winter season (December, January, February and March), grids DVC1, DVC2 and DVC4 show an increasing trend in the mean monthly maximum temperature for the months of December, February and March, and a decrease in the month of January, but it is not statically significant in any month. The DVC3 and DVC5 grids show a decreasing trend in the mean maximum temperature for all months of the winter season and is statistically significant in the month of January ($p < 0.1$) for both grids. The summer season also shows a decreasing temperature but is not statistically significant. Overall, it was observed from the analysis that there was an increase in the mean monthly maximum temperature over the region, especially in the monsoon and winter seasons.

Table 5. Summary of trend analysis for mean monthly maximum temperature using Mann–Kendall nonparametric test.

Month	DVC1			DVC2			DVC3			DVC4			DVC5		
	β	Z	*p*	B	Z	*p*	β	Z	*p*	β	Z	*p*	β	Z	*p*
Jan	−0.011	−0.776		−0.022	−1.226		−0.041	−2.574	**	−0.027	−1.526		−0.040	−2.520	**
Feb	0.029	1.158		0.014	0.599		−0.005	−0.218		0.123	0.586		−0.005	−0.150	
Mar	0.011	0.463		0.001	0.095		−0.140	−0.504		0.006	0.327		−0.009	−0.422	
Apr	−0.006	−0.286		−0.022	−0.940		−0.040	−1.471		−0.016	−0.640		−0.035	−1.253	
May	−0.001	−0.027		−0.013	−0.354		−0.022	−0.695		−0.008	−0.422		−0.012	−0.272	
Jun	−0.002	−0.014		−0.002	−0.054		0.006	0.163		−0.004	−0.095		0.008	0.150	
Jul	0.028	1.716	*	0.024	1.580		0.018	1.376		0.027	1.675	*	0.026	1.812	*
Aug	0.008	0.940		0.012	1.335		0.012	1.226		0.012	1.526		0.012	1.376	
Sep	0.010	1.090		0.007	0.667		0.001	0.041		0.010	0.994		0.005	0.477	
Oct	−0.010	−0.667		−0.016	−1.062		−0.030	−1.716	*	−0.013	−0.926		−0.020	−1.131	
Nov	0.027	1.839	*	0.017	1.321		−0.003	−0.027		0.009	0.763		0.006	0.531	
Dec	0.018	1.294		0.007	0.640		−0.011	−0.831		0.004	0.272		−0.011	−0.872	

Note: *, ** indicate mean significance levels at $p < 0.1$, $p < 0.05$; Z is statistics of Mann–Kendall test; β is the slope estimator.

The results of the Mann–Kendall test for the mean monthly minimum temperature over the Damodar catchment are presented in Table 6, which indicates that the climate of the region was warmed during 1970–2005. The grids DVC3 and DVC5 show an increasing trend for all months except for January (both the grids) and April for grid DVC3. It was found that the increase in the temperature was statistically significant for the months of

February, March, July, August, September and December ($p < 0.05$) in grids DVC3 and DVC5. During the winter season (December, January, February and March), January shows a decrease and February shows an increase in the mean monthly minimum temperature for all the grids but is only statistically significant ($p < 0.05$) for February. While the monthly minimum temperature in March shows an increasing trend for all the grids except for DVC1, this increase is significant only for grids DVC3 and DVC5. The month of December shows a decrease in grids DVC1 and DVC4, and the rest of the grids show an increase in the mean monthly temperature.

Table 6. Summary of trend analysis for mean monthly minimum temperature using Mann–Kendall nonparametric test.

Month	DVC1			DVC2			DVC3			DVC4			DVC5		
	B	Z	*p*	B	Z	*p*	β	Z	*p*	β	Z	*p*	β	Z	*p*
Jan	−0.027	−1.090		−0.021	−1.035		−0.011	−0.436		−0.023	−1.566		−0.014	−0.667	
Feb	0.006	0.313		0.012	1.035		0.029	2.207	**	0.011	0.708		0.034	2.820	**
Mar	−0.006	−0.436		0.011	0.981		0.024	1.839	*	0.007	0.449		0.031	2.193	**
Apr	−0.020	−1.171		−0.004	−0.259		−0.003	−0.191		−0.172	−1.062		0.003	0.136	
May	−0.019	−1.076		−0.006	−0.204		0.009	0.368		−0.016	−0.981		0.018	1.144	
Jun	−0.025	−1.539		−0.007	−0.667		0.007	0.749		−0.017	−1.389		0.009	1.226	
Jul	−0.005	−0.586		0.007	0.831		0.021	2.452	**	0.001	0.054		0.025	2.765	**
Aug	−0.008	−0.994		0.009	1.512		0.024	3.242	**	−0.005	−0.681		0.026	3.201	**
Sep	−0.008	−1.158		0.006	0.899		0.015	2.329	**	−0.007	−0.722		0.020	2.438	**
Oct	−0.013	−0.940		−0.002	−0.150		0.013	0.953		−0.013	−0.885		0.016	1.103	
Nov	−0.019	−0.872		−0.008	−0.259		0.014	0.558		−0.016	−0.967		0.012	0.627	
Dec	−0.009	−0.477		0.002	0.041		0.021	1.430		−0.001	−0.082		0.022	1.648	*

Note: *, ** indicate mean significance levels at $p < 0.1$, $p < 0.05$; Z is statistics of Mann–Kendall test; β is the slope estimator.

During the monsoon season (JJAS), it is observed from grids DVC2, DVC3 and DVC5 that there is an increase in the minimum temperature over the region, which is statistically significant at a 5% level for grids DVC3 and DVC4 in the months of July, August and September. While grids DVC1 and DVC4 show a decrease in the mean monthly minimum temperature, it is not statistically significant. During the summer and post-monsoon season, an increase in the mean minimum temperature is observed for grids DVC3 and DVC5, and a decrease is observed for grids DVC1, DVC2 and DVC4, but again, they are statistically insignificant. Overall, it was found that during 1970–2005, there was an increase in the mean monthly minimum temperature in the region.

3.6. Historical Changes in Water Availability: Reservoir Inflow

The historical changes in the water availability, in terms of the Panchet reservoir inflow, were analyzed by using historical LULC (1972, 1990 and 2001) and decadal climate (1971–1980, 1981–1990 and 1991–2000) information. The analysis shows the impact of the LULC change and climate variability on hydrology in a historical time frame. The analyzed LULCs of 1972, 1990 and 2001 were used to represent the LULC patterns of the 1980s, 1990s and 2000s, respectively, forming a total of nine scenarios, as shown in Table 7. The model was run for each scenario to simulate the reservoir inflow for the Panchet reservoir, and the results are summarized in Table 7. The simulated results were used to compare the effects of LULC as well as climate variability on the Damodar catchment. The measured average annual reservoir inflows for the periods of 1971–1980, 1981–1990 and 1991–2001 were used to compare the observed and simulated reservoir inflows. In Table 7, the difference between T1, T2 and T3 (T4, T5, T6 and T7, T8, T9) indicates the influence of LULC change on the reservoir inflow among the three periods, and T1, T5 and T9 represent the historical change in the reservoir inflow because of the combined effect of LULC change and climate variability. The differences between T1, T4 and T7 indicate the influence of climate variation on the Panchet reservoir. As seen in Table 7, in comparison with T1, the simulated reservoir inflow in T9 increases by 40.44 m^3/s, which represents the combined effect of LULC and climate variability. The land use change during the 2000s (T3) shows an increasing impact on the reservoir inflow by 3.82 m^3/s, which accounts for a 2.47% increased inflow compared to LULC during the 1980s. The contrast between T1, T4 and T7 indicate the influence of climate variation. The climate variation during the 1990s increased the reservoir inflow by 6.99 m^3/s, which accounts for a 4.52% increase from the 1980s. These results thus show that LULC change and climate variability during the 1980s, 1990s, and 2000s increased the reservoir inflow, but the contribution of climate variability was greater than LULC change, as seen in the results.

Table 7. Simulated average annual reservoir inflow to Panchet reservoir under different LULC and climate scenarios.

Scenarios	Land Use	Climate	Measured Inflow (m^3/s)	Simulated Inflow (m^3/s)	Change in Inflow (m^3/s)	Change (%)
T1	1972	1971–1980	153.22	154.56	-	-
T2	1990	1971–1980	-	157.60	3.04	1.97
T3	2001	1971–1980	-	158.38	3.82	2.47
T4	1972	1981–1990	-	161.55	6.99	4.52
T5	1990	1981–1990	158.54	162.57	8.01	5.18
T6	2001	1981–1990	-	163.07	8.51	5.51
T7	1972	1991–2000	-	193.55	38.99	25.23
T8	1990	1991–2000	-	194.27	39.71	25.69
T9	2001	1991–2000	191.69	195.00	40.44	26.16

4. Conclusions

The Soil and Water Assessment Tool model was used to simulate the runoff and reservoir inflows in the Damodar catchment for four independent watersheds and three reservoirs. The simulation results of the model indicate that the monthly runoff from the watersheds and the inflow to the reservoirs are in reasonable agreement with the observed counterparts with a PBIAS of less than ±16.77%. The low RMSE values of the runoff (from 7.60 to 23.06 mm) and reservoir inflows (from b/w 7.84 to 93.90 m^3/s) indicate that the model well simulates the observed values during the calibration and validation periods. On the other hand, higher values of R^2 (varying between 0.81 and 0.95) and NS (varying from 0.74 to 0.93) indicate that the model well simulates the pattern and peaks of the watershed runoff and reservoirs' inflow corresponding to the observed counterparts. LULC prepared from Landsat images revealed that the land cover pattern of the study area changed from 1972 to 2001. The agricultural land (26.71%), water body (88.42%) and settlement (140%) area increased, whereas the forest (15.28%) and wasteland (32.63%) area decreased during the same period. The implication of LULC and climate variability on historical changes in water availability, in terms of reservoir inflow, was analyzed by using historical LULC (1972, 1990 and 2001) and decadal (1971–1980, 1981–1990 and 1991–2000) climate information, finally developing nine simulation scenarios of the SWAT model. It was found from the analysis that the reservoir inflow to the Panchet reservoir increased by 26.16% under the influence of climate variability and LULC change, respectively, from 1971 to 2000. The results also indicate that though LULC change and climate variability increased the reservoir inflow from 1971 to 2000, the contribution of climate variability was greater than LULC change in the catchment.

Author Contributions: Conceptualization, S.K. and A.M.; methodology A.M. and S.K; software, S.K. and A.M.; validation, S.K., A.M. and U.K.S.; formal analysis, S.K. and A.M.; investigation, A.M.; resources, A.M.; data curation, A.M.; writing—original draft preparation, S.K.; writing—review and editing, A.M and U.K.S.; visualization, U.K.S.; supervision, S.K.; project administration, A.M.; funding acquisition, S.K. All authors have read and agreed to the published version of the manuscript.

Funding: This research received no external funding.

Institutional Review Board Statement: Not applicable.

Informed Consent Statement: Not applicable.

Data Availability Statement: Data will be made available on request to the corresponding author.

Acknowledgments: The authors are grateful to the Soil Conservation Department, Damodar Valley Corporation, Hazaribagh, Jharkhand, India, and the Indian Institute of Technology, Kharagpur, West Bengal, India, for providing the data and other facilities.

Conflicts of Interest: The authors declare no conflict of interest.

References

1. Tang, Z.; Engel, B.A.; Pijanowski, B.C.; Lim, K.J. Forecasting land use change and its environmental impact at a watershed scale. *J. Environ. Manag.* **2005**, *76*, 35–45. [CrossRef] [PubMed]
2. Kumar, S.; Mishra, A. Specific Erosion Area Identification using HRU Approach for Effective Sedimentation Control in a River Basin. *Water Resour. Manag.* **2015**, *29*, 1749–1756. [CrossRef]
3. Kumar, P.S.; Praveen, T.V.; Prasad, M.A.; Rao, P.S. Identification of Critical Erosion Prone Areas and Computation of Sediment Yield Using Remote Sensing and GIS: A Case Study on Sarada River Basin. *J. Inst. Eng. Ser. A* **2018**, *99*, 719–728. [CrossRef]
4. Yadav, A.; Penke, S. Multi-objective genetic algorithm optimization of artificial neural network for estimating suspended sediment yield in Mahanadi River basin, India. *Int. J. River Basin Manag.* **2020**, *18*, 1–21. [CrossRef]
5. Im, S.; Kim, H.; Kim, C. Assessing the impacts of land use changes on watershed hydrology using MIKE SHE. *Environ. Geol.* **2009**, *57*, 231–239. [CrossRef]
6. Yang, M.; Xu, J.; Yin, D.; He, S.; Zhu, S.; Li, S. Modified Multi–Source Water Supply Module of the SWAT–WARM Model to Simulate Water Resource Responses under Strong Human Activities in the Tang–Bai River Basin. *Sustainability* **2022**, *14*, 15016. [CrossRef]
7. Githui, F.; Mutu, F.; Bauwens, W. Estimating the impacts of land-cover change on runoff using the soil and water assessment tool (SWAT): Case study of Nzoia catchment, Kenya. *Hydrol. Sci. J.* **2009**, *54*, 899–908. [CrossRef]
8. Kashaigili, J.J. Impacts of land-use and land-cover changes on flow regimes of the Usangu wetland and the Great Ruaha River, Tanzania. *Phys. Chem. Earth* **2008**, *33*, 640–647. [CrossRef]
9. Wan, R.; Yang, G. Influence of land/cover change on storm runoff-A case study of Xitiaoxi River Basin in upstream of Taihu Lake Watershed. *Chin. Geogr. Sci.* **2007**, *17*, 349–356. [CrossRef]
10. Teixeira, A.M.; Soares-Filho, B.S.; Freitas, S.R.; Metzger, J.P. Modeling landscape dynamics in an Atlantic Rainforest region. *Implic. Conserv. For. Ecol. Manag.* **2009**, *257*, 1219–1230. [CrossRef]
11. Mango, L.M.; Melesse, A.M.; McClain, M.E.; Gann, D.; Setegn, S.G. Land use and climate change impacts on the hydrology of the upper Mara River Basin, Kenya: Results of a modeling study to support better resource management. *Hydrol. Earth Syst. Sci.* **2011**, *15*, 2245–2258. [CrossRef]
12. Bishop, P.L.; Hively, W.D.; Stedinger, J.R.; Rafferty, M.R.; Lojpersberger, J.L.; Bloomfield, J. A multivariate analysis of paired watershed data to evaluate agricultural best management practice effects on stream water phosphorus. *J. Environ. Qual.* **2005**, *34*, 1087–1101. [CrossRef]
13. Ghaffari, G.; Keesstra, S.; Ghodousi, J.; Ahmadi, H. SWAT-simulated hydrological impact of land-use change in the Zanjanrood Basin, Northwest Iran. *Hydrol. Process.* **2010**, *24*, 892–903. [CrossRef]
14. Fenicia, F.; Savenije, H.H.G.; Avdeeva, Y. Anomaly in the rainfall-runoff behavior of the Meuse catchment. Climate, land use, or land use management. *Hydrol. Earth Syst. Sci. Discuss.* **2008**, *5*, 1787–1819.
15. Agarwal, S.; Patil, J.P.; Goyal, V.C.; Singh, A. Assessment of Water Supply–Demand Using Water Evaluation and Planning (WEAP) Model for Ur River Watershed, Madhya Pradesh, India. *J. Inst. Eng. Ser. A* **2019**, *100*, 21–32. [CrossRef]
16. Bathurst, J.C.; Ewen, J.; Parkin, G.; O'Connell, P.E.; Cooper, J.D. Validation of catchment models for predicting land-use and climate change impacts, Blind validation for internal and outlet responses. *J. Hydrol.* **2004**, *287*, 74–94. [CrossRef]
17. Li, K.Y.; Coe, M.T.; Ramankutty, N. Investigation of hydrological variability in West Africa using land surface models. *J. Clim.* **2005**, *18*, 3173–3188. [CrossRef]
18. Reshma, T.; Reddy, K.V.P.D.; Agilan, V. Parameters Optimization using Fuzzy Rule Based Multi-Objective Genetic Algorithm for an Event Based Rainfall-Runoff Model. *Water Resour. Manag.* **2018**, *32*, 1501–1516. [CrossRef]
19. Patil, N.S.; Nataraja, M. Effect of land use land cover changes on runoff using hydrological model: A case study in Hiranyakeshi watershed. *Model. Earth Syst. Environ.* **2020**, *6*, 2345–2357. [CrossRef]

20. Twine, T.E.; Kucharik, C.J.; Foley, J.A. Effects of land cover change on the energy and water balance of the Mississippi River basin. *J. Hydrometeorol.* **2004**, *5*, 640–655. [CrossRef]
21. Yuan, F.; Sawaya, K.E.; Loeffelholz, B.C.; Bauer, M.E. Land cover classification and change analysis of the Twin Cities (Minnesota) Metropolitan Area by multitemporal Landsat remote sensing. *Remote Sens. Environ.* **2005**, *98*, 317–328. [CrossRef]
22. Munoth, P.; Goyal, R. Hydromorphological analysis of Upper Tapi River Sub-basin, India, using QSWAT model. *Model. Earth Syst. Environ.* **2020**, *6*, 2111–2127. [CrossRef]
23. Kepner, W.G.; Semmens, D.J.; Bassett, S.D.; Mouat, D.A.; Goodrich, D.C. Scenario analysis for the San Pedro River, analyzing hydrological consequences of a future environment. *Environ. Monit. Assess.* **2004**, *94*, 115–127. [CrossRef]
24. Ma, X.; Xu, J.; Luo, Y.; Aggarwal, S.P.; Li, J. Response of hydrological processes to land-cover and climate changes in Kejie watershed, south-west China. *Hydrol. Process.* **2009**, *23*, 1179–1191. [CrossRef]
25. Zhang, Y.; Arthington, A.H.; Bunn, S.E.; Mackay, S.; Xia, J.; Kennard, M. Classification of Flow Regimes for Environmental Flow Assessment in Regulated Rivers: The Huai River Basin, China. *River Res. Appl.* **2011**, *28*, 989–1005. [CrossRef]
26. Ahiablame, L.; Sheshukov, A.Y.; Mosase, E.; Hong, J. Modelling the impacts of grassland to cropland conversion on river flow regimes in Skunk Creek watershed, Upper Midwest United States. *River Resear. Appl.* **2019**, *35*, 1454–1465. [CrossRef]
27. Palamuleni, L.G.; Ndomba, P.M.; Annegarn, H.J. Evaluating land cover change and its impact on hydrological regime in Upper Shire River catchment, Malawi. *Reg. Environ. Chang.* **2011**, *11*, 845–855. [CrossRef]
28. Nie, W.; Yuan, Y.; Kepner, W.; Nash, M.S.; Jackson, M.; Erickson, C. Assessing impacts of Landuse and Landcover changes on hydrology for the upper San Pedro watershed. *J. Hydrol.* **2011**, *407*, 105–114. [CrossRef]
29. Yan, B.; Fang, N.F.; Zhang, P.C.; Shi, Z.H. Impacts of land use change on watershed streamflow and sediment yield: An assessment using hydrologic modelling and partial least squares regression. *J. Hydrol.* **2013**, *484*, 26–37. [CrossRef]
30. Narsimlu, B.; Gosain, A.K.; Chahar, B.R. Assessment of Future Climate Change Impacts on Water Resources of Upper Sind River Basin, India Using SWAT Model. *Water Resour. Manag.* **2013**, *27*, 3647–3662. [CrossRef]
31. Qi, S.; Bao, W.; Shi, P.; Yu, Z.; Li, P.; Zhang, B.; Jing, P. Evaluation of runoff responses to land use changes and land cover changes in the upper Huaihe river basin, China. *J. Hydrol. Eng.* **2012**, *17*, 800–806.
32. Arnold, J.G.; Srinivasan, R.; Muttiah, R.S.; Williams, J.R. Large area hydrologic modeling and assessment, part I: Model development. *JAWRA* **1998**, *34*, 73–89. [CrossRef]
33. Neitsch, S.L.; Arnold, J.G.; Kiniry, J.R.; Williams, J.R. *Soil and Water Assessment Tool Theoretical Documentation*; Texas Water Resources Institute: College Station, TX, USA, 2005.
34. ASCE. Criteria for evaluation of watershed models. *J. Irrig. Drain. Eng.* **1993**, *119*, 429–442.
35. Fu, G.; Charles, S.P.; Yu, J.; Liu, C. Decadal climatic variability, trends and future scenarios for the North China Plain. *J. Clim.* **2009**, *22*, 2111–2123. [CrossRef]
36. Moriasi, D.N.; Arnold, J.G.; Van Liew, M.W.; Bingner, R.L.; Harmel, R.D.; Veith, T.L. Model evaluation guidelines for systematic quantification of accuracy in watershed simulation. *Trans. ASABE* **2007**, *50*, 885–900. [CrossRef]